# Fullerenes and their nonlinear optical properties

Kailash C Rustagi

Centre for Advanced Technology, Indore-452 013, India

**Abstract** : Nonlinear optical properties of fullerenes are reviewed after a brief overview of their other physical properties. Available information on synthesis and purification of various fullerenes and fullerene derivatives is given first. This is followed by a review of their atomic and electronic structure, and experimental results on their linear and nonlinear optical response Finally, we summarize theoretical results on their hyperpolarizability in the background of available experimental information.

## 1. Introduction

Since the discovery [1] two years ago of a simple method of synthesizing cage–like carbon molecules—now commonly called fullerenes—there has been an explosive growth in the study of their physical and chemical properties. This brief overview attempts a critical examination of the available information on their physical properties with special reference to understanding their nonlinear optical response.

Much has been written about the history of the discovery of Buckminsterfullerene $C_{60}$ and its *tricontahedron* or truncated icosahedron structure [2] which resemble a football. The story has been told by the main participants [3–6] in the drama as well as by others [7]. The impact of this new family of molecules has been felt in many branches of physics and chemistry, but perhaps none more than the relatively new area of atomic clusters.

The commonest experiment in cluster physics involves photoionization of a molecular beam consisting of clusters of various sizes and then detecting their mass spectra. It was in such an experiment on sodium clusters some years ago [8] that it was found that clusters containing 2, 8, 20, 40, 58 and 92 atoms were conspicuously more abundant than their

neighbours in the mass spectrum. By making the ionizing laser tunable and recording the abundance spectra as a function of the wavelength $\lambda$ one can also obtain the ionization potential as function of the cluster size [9]. For metal clusters, the occurrence of such magic numbers can be understood in terms of a simple spherical cluster model [8–10]. However, in general, the calculation of ionization potentials or cohesive energies without any *a priori* information of the structure is a very challenging job because one must simultaneously obtain the atomic positions too by minimising the total free energy. For relatively small clusters, near first principle calculations are now possible while for larger clusters appropriate theories are still being developed.

Since carbon has a strong tendency to form directed covalent bonds, one might expect that carbon clusters would show different magic numbers and eventually at large sizes stabilize into an approximate diamond or graphite structure. However, when—motivated by the need to understand the possible role of large carbon clusters in outer space—the experiments were actually done at Rice University the results turned out to be far more surprising. When hot carbon gas produced by laser evaporation of graphite condensed in the presence of helium, under some experimental conditions the mass spectrum of clusters contained one dominant peak corresponding to $C_{60}$. This indicated that the cluster $C_{60}$ is much more stable than other clusters. Kroto *et al* [2] looked for possible structures that a $C_{60}$ molecule could have and hit upon the idea of the truncated icosahedral structure in which all the carbon atoms are identical and all the valence can be satisfied. Since the structure also has many 'resonances', it could be expected to be very stable. Several theoretical papers reported calculations of the electronic, vibrational and optical properties of $C_{60}$ assuming this proposed structure; yet investigation of, and belief in the existence of this fascinating molecule tended to stagnate due to lack of a suitable method of synthesizing $C_{60}$ in sufficient quantities. The first reports [1,11] of accumulating macroscopic quantities of $C_{60}$ came towards the end of 1990.

This discovery [1] started the explosive growth of scientific research in fullerenes. For the cluster physics community it has brought home the point that new useful materials can be synthesized by condensation of hot gases. In addition to fullerenes new cage-like molecules called metallo-carbohedrenes [12] have also been synthesized during the last year. The second lesson is that chemical arguments may play an important role in envisaging possible structures. It has also emerged that one should use thermodynamic arguments with some caution. Graphite is the most stable form of carbon as it has the maximum cohesive energy per atom. Yet, we all know that diamond and now fullerite are quite stable and useful forms of carbon. There are several strands of the work on fullerenes—several physical properties of these novel molecular solids are being explored vigorously. Some of them are described briefly in the following two sections. In Section 4, we discuss the electronic structure and the linear optical properties of fullerenes. Experimental work on nonlinear optical properties is surveyed in Section 5 and theory of the nonlinear polarizabilities in Section 6. Finally in conclusion, we discuss the prospects of fullerenes as nonlinear optical materials.

Obviously many interesting aspects of fullerene research are omitted in this review. Fortunately, there are several conference proceedings [13–15] and special issues of journals [16] and other reviews [17] available which cover various aspects of this research.

One of the most important areas omitted completely is the study of the superconducting response of alkali-doped fullerites with relatively high transition temperatures. Although at present the fullerene based superconductors do not appear to be the most promising high $T_c$ superconductors, understanding their superconductivity is considered very important because of their molecular binding. Several relevant articles can be found in the reviews cited above.

## 2. Synthesis and purification

Although many methods of synthesizing fullerenes have been reported, so far the simplest and most successful is still the original Krätschmer–Huffmann technique [1]. First, the carbon soot is prepared by striking a contact arc discharge in He atmosphere at 100–300 torr. Before filling the system with He, it is desirable to evacuate the chamber to $10^{-5} - 10^{-6}$ torr to avoid contamination. To maintain the discharge, one has to ensure that the contact between the electrodes is not lost as the tips of the electrode wear out due to loss of material by evaporation. This can be done either manually or by spring loading one of the electrodes. The evaporated carbon is collected on a cooled copper foil, scraped and then washed in ether to remove any hydrocarbons that may be present. Benzene or toluene soluble part of the soot is then extracted by using a standard Soxhlet apparatus. This extract contains many fullerenes. $C_{60}$ can be separated by sublimation and more commonly by liquid chromatography. Further separation by high performance liquid chromatography has also yielded several higher fullerenes in reasonably large quantities [18], specially $C_{70}$, $C_{76}$, $C_{78}$ and $C_{84}$. Methods of separation and purification are being continuously improved. In particular, several improvements in the liquid chromatography have been reported recently [19]. Apart from the arc method, macroscopic quantities of fullerenes can also be generated by modifying the laser-evaporation method originally used by Smalley's group. If the laser evaporation is done at 1200 C and at 100–300 torr pressure of an inert gas as much as 10% of the vaporized carbon converts into fullerenes. The method has been used for making doped fullerenes also [20] and may be worth trying to explore the possibility of forming cage-like compounds of other materials.

Ever since macroscopic quantities of $C_{60}$ became available, attempts have been made to obtain its chemical derivatives. Probably the most exciting such effort has been to dope the solid fullerite with metal ions like K, Na, Rb and Cs. Solids of the form $M_3C_{60}$ are superconducting with $T_c$ ranging from 2 K to 33 K [21]. The highest $T_c$ reported for a fullerite superconductor is 45 K for Rb–Tl doped $C_{60}$. As already noted in the introduction this important part of fullerene research will not be discussed in this review. In these materials metal ions occupy intersticial sites between the bucky balls. In fullerenes a novel possibility

of doping exists : one can put atoms, molecules or clusters inside the cage (endohedral complexes). Modification of the cage itself by substitution or attachment of radicals is also possible. With these 3 types of doping possible, a new notation was suggested by Smalley [20] and has been commonly accepted. $A_n$ @$C_{60}$ denotes the molecule $C_{60}$ which contains $n$ atoms of the element A inside the cage ; $C_{59}B$ denotes a molecule which has one of the carbon atoms substituted by Boron etc. Although the formation of $C_{59}B$, $C_{58}B_2$ [20] and several nitrogen derivatives [22] was reported quite some time back, no further results seems to have been reported on these very interesting molecules. It appears that they are difficult to produce in macroscopic quantities.

Since fullerenes provide 3-dimensional $\pi$-electron clouds in various shapes, it is clear that they will give rise to a new branch of chemistry. Considerable progress has already been reported and much more may be expected in near future [23].

## 3. Structure

The best known fullerene structure is of course that of $C_{60}$, the Buckminsterfullerene *i.e.*, all the atomic positions are quite well known experimentally and have been well corroborated by theory. The X-ray diffraction data is consistent with the truncated icosahedron structure shown in Figure 1 along with the parent icosahedron. The twelve vertices of the complete
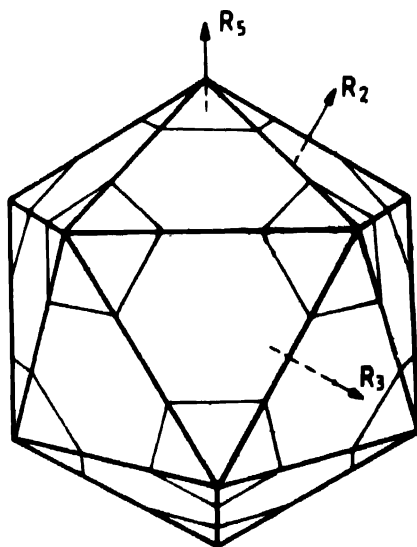


**Figure 1.** The truncated icosahedron structure of $C_{60}$ along with the complete icosahedron. Symmetry axes of the icosahedron are also shown.

icosahedron have the same angular coordinates as the centres of the twelve pentagons in the $C_{60}$ structure. The distance of the centre of the pentagonal faces from the centre of $C_{60}$ determines the ratio of the long bond or pentagonal edge to the short bond or the edge shared

between two hexagons. When these two edges are equal the coordinates of the vertices of the truncated icosahedron are given by [24]

$$\alpha(0, \pm1/2, \pm3\tau/2), \quad \alpha(\pm\tau/2, \pm1, \pm(2\tau+1)/2), \quad \alpha(\pm\tau, \pm1/2, \pm(2+\tau)/2)$$

and their cyclic permutations ; $\alpha$ here is the distance between two neighbouring vertices and $\tau = \left(1 + \sqrt{5}\right)/2$ is the golden ratio. The radius of the sphere in this case is $\alpha(1 + 3\tau/4)$. The structure of $C_{60}$ is obtained by effecting the truncation slightly closer to the centre such that the average bond length equals $\alpha$; the hexagon-hexagon bonds are then a bit shorter than the pentagon–hexagon ones. High resolution NMR spectra [25] give the two bond lengths as $1.40 \pm 0.015$ Å and $1.45 \pm 0.015$ Å. This is consistent with the other structure determinations such as X-ray diffraction [24] in the solid state.

The availability of experimental data on the structure has provided an excellent check on the reliability of various methods of calculation for the structure of clusters. For example, the most reliable and most sophisticated such calculations [26] using the Car–Parinello method [27] with the local density approximation and angular momentum dependent pseudopotentials, yield 1.39 Å and 1.45 Å as the two C–C distances in a free $C_{60}$ molecule. Using the same technique the calculated phonon frequencies are in reasonable agreement with the experimental values [26].

For $C_{70}$, it is known that the molecule has $D_{5h}$ symmetry and 8 inequivalent C–C bond lengths. The simplest way to visualize the $C_{70}$ structure is to divide the $C_{60}$ structure into two equal halves and rotate one half relative to the other by $\pi/10$ about the axis joining the centres of two opposite pentagons. Ten more atoms are now added along the equator so as to introduce 5 additional hexagonal faces at the equator. Thus, as we go from top to bottom we have successive layers with a pentagonal face, 5 hexagonal faces, 5 pentagonal faces, 5 hexagonal faces, 5 hexagonal faces, 5 hexagonal faces, 5 pentagonal faces, 5 hexagonal faces and a pentagonal face at the bottom. The $xy$ plane is one mirror-symmetry, there is a five fold rotation about the $z$-axis joining the centres of top and bottom pentagons and there is a mirror plane containing the $z$ axis. The bond lengths may now be relaxed so that these symmetry elements ($D_{5h}$ symmetry) are preserved. This allows only 8 independent bond lengths which can be identified as follows. All the five bonds in the top (and bottom) pentagon are equal because of the 5 fold axis. This is bond type 8 in Table 2 of McKenzie *et al* [28] and there are 10 of these. Next, there are 10 bonds connecting top (bottom) pentagons to next row of pentagons. This is bond type 7 of Ref. [28]. Bond type 6 is a pentagon edge as are bond type 3 and 4 which all belong to the next layer of pentagons. They need not be equal since they are not connected by any symmetry element of $D_{5h}$ group. The bonds of type 5 connect two pentagons while those of type 2 connect a hexagon and a pentagon. Type one bonds connect hexagons of top and bottom halves and are absent in the $C_{60}$ structure. Mckenzie *et al* analysed their electron diffraction data to conclude that the bond lengths of all types except 1 are close to the corresponding bond lengths in $C_{60}$ while type 1 bonds have a length

$1.41^{+0.03}_{-0.01}$A. Their values for bond lengths $r_2$ to $r_8$ are in quite good agreement with the calculated values of Andreoni *etal* [29] and Saito and Oshiyama [30] using the LDA as well as with those of Wang *et al* [31] using a tight binding calculation. For the type 1 bond, however, the theoretical values vary noticeably. While Andreoni *et al* [29] give this bond length to be 1.467 Å and Wang *et al* 1.452 Å, Saito and Oshiyama [30] used the LDA method with norm-conserving pseudopotential to estimate this bond length to be 1.42 Å much closer to the experimental estimate. Although the experimental analysis also indicates a larger uncertainty of the larger bond length side, McKenzie *et al* have noted that this bond length is close to that in graphite. More accurate experimental estimates of these bond lengths will be very useful in establishing the relative reliability of various methods of calculation in cluster physics.

Interest in the structure of higher fullerenes emanates from the fact that many of them are expected to have a relatively lower symmetry mainly because of topological constraints. Almost all the fullerenes between $C_{76}$ and $C_{94}$ have symmetries without the five fold axes.
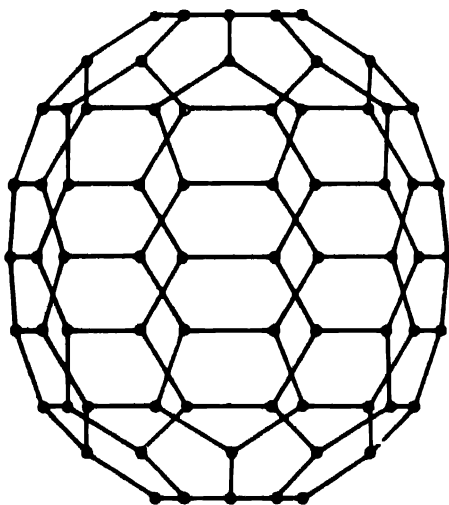


**Figure 2.** The structure of $C_{70}$.

More interestingly, several are expected to be nearly equally stable in more than one structure. By comparing the experimental NMR spectra with those expected for each symmetry species, Kikuchi *et al* [32] concluded that $C_{78}$ consists of 3 isomers with symmetry $C_{2v}$, $C_{2v}$ and $D_3$ in the ratio 5 : 2 : 2 while Diederich *et al* [33] found that their sample had molecules with $C_{2v}$ and $D_3$ structures in the ratio of 5 : 1. Similarly, $C_{84}$ was found to have [32] only two isomers with symmetry $D_2$ and $D_{2d}$ although as many as 24 were considered possible at one stage. Wang *et al* [34] have shown that only two isomers with symmetry $D_2$ and $D_{2d}$ respectively are energetically favoured. Overall, one can expect that as more and more experimental data becomes available, one would know the structure of higher fullerenes also as accurately as $C_{60}$. Simultaneously, methods have to be found to separate the various isomers. We have

described the available information about the structure of various molecules in some detail since we anticipate that several of them are potentially good molecules for nonlinear optical applications.

Fullerenes are stable and weakly interacting molecules. The attractive interaction between the molecules is Van der Waal's type if the molecule does not have an electric dipole moment in the ground state. In the first announcement of synthesizing macroscopic amounts of $C_{60}$, Krätschmer *et al* [1] also showed that a new solid state form of carbon can be formed—it is crystalline, has a density of 1.65 and a refractive index of $\approx 2$. The crystal structure was originally thought to be hexagonal closed packing but has later turned out to be much more interesting. It is now generally agreed that at room temperature the crystal structure is a rotationally disordered *fcc i.e.*, at each lattice point of the *fcc* lattice a $C_{60}$ molecule is located. However, the orientations of the molecules are not correlated at room temperature. As the temperature is reduced, a phase transition is observed at 249 K [35]. The low temperature phase is a simple cubic structure with 4 $C_{60}$ molecules per unit cell and has the space group $Pa\bar{3}$. The basic orientational ordering behaviour was explained in a phenomenological model by Lu *et al* [36]. They argue that because of the two different bond lengths there is a relative deficiency of electrons at the single bonds and a corresponding excess at the double bonds. Denoting by $q$ the effective charge on a single bond and by charge neutralisation $-2q$ on a double bond, they postulate the interaction between two bucky balls as

$$V_{12} = \sum_{i,j=1}^{60} 4\,\varepsilon \left[ \left( \frac{\sigma}{|r_{1i} - r_{2j}|} \right)^{12} - \left( \frac{\sigma}{|r_{1i} - r_{2j}|} \right)^{6} \right]$$
$$+ \sum_{m,n=1}^{90} \frac{q_m\,q_n}{|b_{1m} - b_{2n}|} \tag{1}$$

where $r_{1i}$, $r_{2j}$ are the coordinates of C atoms, $b_{1m}$, $b_{2n}$ those of bond centres and $q_m$, $q_n$ are the effective bond charges. Using this model potential Lu *et al* [36] found that solid fullerite undergoes a first order phase transition at 270 K (experimentally 249 K) from the high temperature *fcc* structure to the ordered $Pa\bar{3}$ structure. The calculated pressure dependence of the transition temperature is also in good agreement with the experimental observations. The orientational ordering of $C_{60}$ and $C_{70}$ crystals has since attracted a lot of attention [37]. As higher fullerenes become available in macroscopic quantities much more excitement is expected.

## 4. Electronic structure and linear optical properties

The fascinating structure for the extra stable $C_{60}$ cluster proposed by Kroto *et al* [2] drew the attention of many theoreticians. Since each atom is bonded to three others, the fourth electron has a wavefunction similar to the $\pi$ electron orbital in graphite or benzene with some

modification due to the bending of the $\sigma$-electron network. The earliest calculations using the Hückel theory [38], CNDO/S method [39] and the linear muffin–tin orbital (LMTO) method [40] provided a rather good starting point. In fact, one of these early predictions of optical spectra played an important role [41] in discovering a method of producing $C_{60}$. Since $\pi$–electrons are expected to be delocalized over the surface defined by the $\sigma$–electron network, they can be treated in a nearly free–electron model [42–44]. In this model as in the empirical pseudopotential method [45] for semiconductors, we first make an 'empty lattice' description for the $C_{60}$ molecule and then treat the icosahedral pseudopotential perturbatively. The 'empty lattice' in this case has spherical symmetry, and we take this zeroth order model to be 60  $\pi$–electrons confined in a spherical shell of mean radius $R = 3.55$ Å and thickness $t \simeq 3$ Å, consistent with other estimates of the electron density. The eigenfunctions for this system are [43]

$$\phi_{nlm}(r) = f_{nl}(r)\, Y_{lm}(\theta,\phi),$$  (2)

with        $$f_{nl}(r) = N\left( j_l(k_{nl}r) - \frac{j_l(k_{nl}R_-)}{y_l(k_{nl}R_-)}\, y_l(k_{nl}r) \right),$$  (3)

where $j_l$ and $y_l$ are the spherical bessel and neumann functions and $Y_{lm}(\theta,\phi)$ denote the spherical harmonics. $N$ is the normalization constant, $k_{nl}$'s are determined by $f(R_+) = 0$, and $R_{\pm} = R \pm t/2$ are the outer and inner radii of the shell. The energy levels are given by

$$E_{nl} = \frac{\hbar^2}{2m}\, k_{nl}^2.$$  (4)

The energy levels are well approximated by [43]

$$E_{nl} = (\hbar^2/2m)\left( \frac{n^2\pi^2}{t^2} + \frac{l(l+1)}{R^2} \right),$$  (5)

$n$ and $l$ being the radial and angular quantum numbers. As shown in Figure 3, the $n = 1$ radial functions are nodeless whereas the $n = 2$ radial functions have a node near $r = R$. Since ideally the $\pi$–electrons have vanishingly small overlap with the $\sigma$–electron skeleton, we choose them to occupy the $n = 2$, $l = 0$ to 5 energy levels. The $n = 1$ levels which lie below the $n = 2$, $l = 0$ level have maximum charge density at $r = R$ and are assumed to he filled by the $\sigma$–electrons. The $\sigma$–electrons are expected to have a much smaller radial spread than the $\pi$-electrons. Thus, the relative position of the $\sigma$ and $\pi$ levels is not expected to be accurately depicted by our model potential having a uniform radial width. On the other hand, the total band width occupied by $\sigma$–electrons or $\pi$–electrons does not depend on this width and is well depicted by our model potential. Later calculations [46] using the spherical jellium model have shown that $\sigma$–electrons indeed occupy $n = 1$, $l \leq 12$ levels with $l = 11$ and 12 partially occupied.

The 22–fold degenerate (including spin degeneracy factor), $l = 5$ level is partially occupied by 10 electrons so that the $\pi$–electron structure is sensitive to all perturbations which split this level. The perturbation due to the presence of the 60–vertex $\sigma$–electron skeleton has
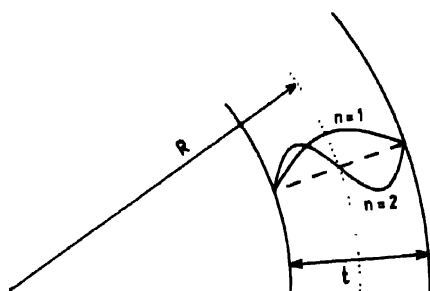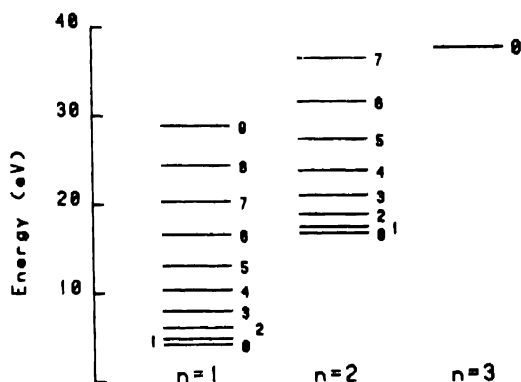


**Figure 3.** The energy levels and wavefunctions for the empty lattice corresponding to $C_{60}$ [from Ref 43].

icosahedral symmetry [47] (group $I_h$) which splits the $l = 5$ level into 3 levels of $t_{1u}$, $t_{3u}$ and $h_u$ symmetry. To calculate the energy levels and the wavefunctions we proceed in the spirit of the empirical pseudopotential method (EPM) for semiconductors. We find that the radial wavefunctions are nearly independent of $l$, so that corresponding to the plane waves in the EPM, our unperturbed states are $f_{n=2}(r) Y_{lm}(\theta,\phi)$. The icosahedral perturbing potential can also be expanded into a series of spherical harmonics. Only those $l$ values will occur in the expansion which contain the identity representation of the icosahedral group $I_h$. Since the levels closest to the Fermi level have either $l = 5$ or $l = 6$, it suffices to retain only the $l = 6$, 10 and 12 components of the potential. The $l = 0$ term could be ignored because it is a constant. The next non zero contribution comes from $l = 16$. Thus to see the effect of the icosahedral perturbation $V$ in the $n = 2$ subspace one can write,

$$\langle lm|V|l'm'\rangle = A_6 \langle lm|V_6|l'm'\rangle + A_{10}\langle lm|V_{10}|l'm'\rangle + A_{12}\langle lm|V_{12}|l'm'\rangle \qquad (6)$$

where $V_6$, $V_{10}$ and $V_{12}$ are those linear combinations of $l = 6$, 10 and 12 spherical harmonics, respectively, which remain invariant under the opeiations of $I_h$ [43]. The $\pi$–electron energy levels are then obtained by diagonalising the hamiltonian numerically.

The use of a rigid confining shell in the zeroth order approximation makes the separation between energy levels of different $l$ values somewhat larger than that expected from a more realistic spherically averaged jellium potential [46]. The effect of the icosahedral pseudopotential is mainly to split the multiplets of a given $l$. So we fix the pseudopotential parameters such that the splitting of the $l = 5$ empty lattice level gives a HOMO–LUMO gap of 1.8 eV and the lowest electric–dipole allowed transition occurs at $\simeq 3.7$ eV. This leaves one parameter free which is chosen to minimize the discrepancy with the next optical absorption peak. Inspite of the simplicity of our starting spherically symmetric potential, our calculated energy levels show reasonable agreement with the valence photo–ionization spectrum [43,44]. The values of the parameters used are $A_6 = -0.035$ Ry, $A_{10} = 0.4$ Ry and $A_{12} = 0.15$ Ry. Our calculated $\pi$-electron density shows a much stronger concentration over the $\sigma$-bond skeleton than that obtained in the zero-range potential model [44]. The electron density per solid angle at the centre of a hexagon is less than 2 compared to about 5.5 at the centre of a pentagonal edge and about 6.5 at the centre of a bond shared by two hexagons. These estimates are in very good agreement with a recent LDA calculation [46]. It is interesting to note that in the spherical harmonic expansion for the electron density, although the leading correction to the $l = 0$, spherically symmetric term is the $l = 6$ term, its coefficient is substantially smaller than that of the next term with $l = 10$. A good approximation to the electron density can be obtained by retaining only the $l = 0$ and $l = 10$ terms which in our model for the $\pi$-electrons is

$$\rho_\pi(r) = \frac{60}{4\pi} - 3.88 \left| f_2(r) \right|^2 V_{10}(\theta, \phi) \tag{7}$$

where $f_2(r)$ is the normalized radial eigenfunction with $n = 2$ for our empty lattice problem. We have neglected the weak $l$-dependence of $f_2(r)$ as mentioned earlier.

The nearly free electron model is suitable only when the $\pi$ electron cloud has a high symmetry. However, another simple model *viz.*, the tight–binding method earlier used by several authors [48–50] is very appropriate for describing the electronic structure of fullerenes. In the tight-binding model for $C_{60}$ the occupied valence electron states and the lowest few excited states are described by the $240 \times 240$ Hamiltonian matrix in the basis set provided by 240 orthogonal atomic like orbitals—four ($s$, $p_x$, $p_y$, $p_z$) at each atomic site. Since only the nearest neighbour interactions are retained, the only parameters involved in the Hamiltonian are the atomic site energies $E_p$ and $E_s$ which are characteristic of the chemical species occupying the site and the hopping integrals $V_{ss}$, $V_{sp}$, $V_{pp\sigma}$ and $V_{pp\pi}$ which are usually scaled to the corresponding interatomic distance [51]. We have used this model to calculate

the electronic structure and nonlinear optical properties of substituted fullerenes [42,52]. In view of the scaling mentioned above, in our calculations for heteroatom bonds like C–N and C–B the hopping integrals were assumed to differ from the C–C hopping integrals only if the corresponding bond lengths were different. The carbon site energies and C–C hopping integrals were taken from the work of Tománek and Schluter [48] adapted to the more realistic [25] C–C bond lengths $d_1 = 1.40$ Å and $d_2 = 1.45$ Å, respectively for the short and the long bonds. The site energies $E_s$ and $E_p$ for B and N were taken to be $E_s(B) = -2.32$ eV, $E_p(B) = 2.33$ eV, $E_s(N) = -12.82$ eV and $E_p(N) = -2.5$ eV so that site energy differences between C, N and B are the same as those given by the solid–state tables [51]. The calculated energy levels for $C_{60}$, $C_{59}B$ and $C_{59}N$ are shown in Figure 4. In our calculations for $C_{59}B$ and $C_{59}N$ also the C–C bond lengths were taken as 1.40 Å and 1.45 Å and the perturbation of the atomic positions caused by B and N doping was included following the work of Andreoni *et al* [53] *i.e.*, the short bond and the long bonds involving boron are elongated by 10% and 7.5% respectively, leaving the rest of the carbon cage unperturbed. However, to check the robustness of the calculated results we also tried several other values of bond lengths. For $C_{60}$, the $z$–axis was chosen to be a five fold rotation axis while for $C_{59}B$ and $C_{59}N$, it was chosen to pass through the substitution site.

The most noticeable feature of these energy spectra is that in $C_{59}B$ and $C_{59}N$ most of the $n$-fold degenerate levels of $C_{60}$ split into a group of $(n-1)$ closely spaced levels whose energies are almost the same as in $C_{60}$, and a split-off nondegenerate level (apart from spin degeneracy). This is particularly true for those levels having a predominantly $\pi$–electron character. This is mainly because of our assumption that the perturbation caused by the doping of the cage is localized near the dopant atoms. In fact this splitting of an $n$–fold degenerate level in $C_{60}$ into an $(n-1)$ fold and a 1-fold level is strictly true in the Hückel model if the effect of the impurity atom is only to change the site energy, whereas only singly degenerate levels are expected in substituted fullerenes $C_{59}B$ and $C_{59}N$ purely on the basis of molecular symmetry. This is because, in the Hückel model, out of the $n$ linearly independent eigenfunctions of an $n$–fold degenerate level, $(n-1)$ can be chosen to vanish at the impurity site. The corresponding eigenvalues therefore remain unaffected by the localized perturbation caused by the impurity. The remaining one eigenfunction has a large amplitude at the impurity atom and is shifted above or below the unperturbed level depending upon whether the impurity is less or more electro–negative compared to carbon. Thus boron, being less electro–negative compared to carbon, gives rise to a split–off level above the $n-1$ 'unperturbed' levels much like an acceptor level in a semiconductor. Similarly the split–off levels in $C_{59}N$ are like donor levels. We note that the splitting of an $n$–fold degenerate level into $(n-1)$ and 1-fold groups is also seen in the LDA calculations [53]. This indicates the reliability of our calculations using the tight–binding method. The results in Figure 4 also show that the relaxation of the boron atom position increases the shift of the impurity level. The remaining 4 levels of the 5–fold degenerate HOMO level in $C_{60}$ are more split in the LDA calculation

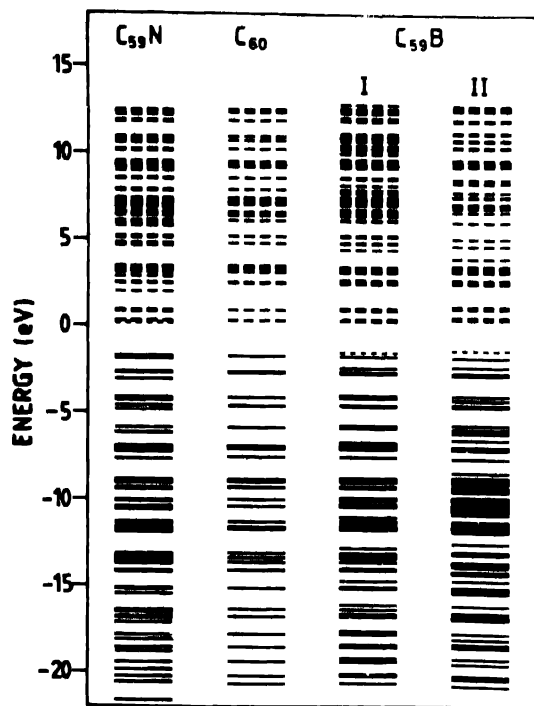than in our calculation presumably because of relaxation of the positions of the carbon atoms in the cage.



**Figure 4.** The electronic energy levels for $C_{60}$, $C_{59}B$ and $C_{59}N$ I . unshifted boron, II . boron atom relaxed

Since $C_{59}B$ has 239 valence electrons and $C_{59}N$ has 241, both have partially filled levels. The lowest gap in both the molecules is the impurity level splitting which is very small but the oscillator strength of this transition is negligible. In $C_{59}B$, the most important new electric–dipole transition is between the two impurity levels split–off from the 2 highest filled $C_{60}$ levels of $h_g$ and $h_u$ symmetry, which we may refer to as the split-off $h_g$ and split-off $h_u$ levels. In $C_{59}N$ the new strong transition is between the impurity levels split–off from the 2 lowest unfilled levels of $C_{60}$ of $t_{1u}$ and $t_{1g}$ symmetry. The corresponding transition energies are 0.9 eV and 0.6 eV in $C_{59}B$ and $C_{59}N$ respectively.

Optical absorption of $C_{60}$ in hexane solution has been measured [54,55] and analyzed in some detail [55]. For the molecule, HOMO–LUMO transition is forbidden and in the emperical pseudopotential model the lowest allowed electric dipole transitions are expected at 3.7, 3.8 and 3.94 eV corresponding to, $g_g \cdot t_{1u}$, $h_u \quad t_{1g}$, and $h_g \rightarrow t_{1u}$ single particle transitions.

While the quantitative agreement is quite good for the various transition energies, that for oscillator strengths is not so satisfactory [55]. Bertsch *et al* [56] have analysed the problem in the random phase approximation and found that the absorption spectra are

strongly modified by the screening of the applied electric field by $\pi$ electrons themselves. A strong resonance very similar to the Mie type plasmon resonance in a metal particle characterises the response at higher energies $\approx 20$ eV [56,57]. Absorption spectra of $C_{70}$ and higher fullerenes have also been measured but a detailed analysis is still awaited. At first sight it appears surprising that in spite of the much reduced symmetry of higher fullerenes, they all have only weak absorption bands in the visible and near infrared. Optical constants of $C_{60}$ fullerite have been also been reported [58] as also the photoemission spectrum [59].

## 5. Experimental observations of optical nonlinearities

For the purpose of this review the nonlinear response of a medium can be divided into two classes depending upon whether or not any energy is absorbed by the medium. If no energy is absorbed, the nonlinear process is passive and can be described in terms of the polarization $P$, i.e., the induced electric dipole moment density in the medium. For a medium consisting of independent molecules—e.g. gases—the induced dipole moment $\mu_1$ can be expanded into a power series in the incident field $E$ [60,61]

$$\mu_i = \alpha_{ij} E_j + \beta_{ijk} E_j E_k + \gamma_{ijkl} E_j E_k E_l + \cdots \tag{8}$$

where the summation over repeated indices is implied, $\alpha_{ij}$ is the linear polarizability tensor and $\beta_{ijk}$ and $\gamma_{ijkl}$ are the second and third order polarizability tensors. $\alpha$ describes the linear optical properties of the molecule while $\beta$, which vanishes in inversion symmetric systems, describes nonlinear optical phenomena such as the electro–optic effect, second harmonic generation and optical rectification. The third order polarizability tensor describes a large variety of phenomena such as the third harmonic generation, four–wave mixing and self interaction of a laser beam. The total polarization of a homogenous molecular medium can be written as [61]

$$P_i = \chi_{ij}^{(1)} E_j + \chi_{ijk}^{(2)} E_j E_k + \chi_{ijkl}^{(3)} E_j E_k E_l + \cdots \tag{9}$$

where

$$\chi_{ij}^{(1)} = N L \alpha_{ij} \tag{10}$$

$$\chi_{ijk}^{(2)} = N L^3 \beta_{ijk}, \tag{11}$$

and

$$\chi_{ijkl}^{(3)} = N L^4 \gamma_{ijkl}. \tag{12}$$

Here $L$, the local field correction factor [61], accounts for the fact that the field seen by a molecule is the applied field modified by that radiated by other molecules. Usually the polarizability $\alpha$, $\beta$ and $\gamma$ and the susceptibilities $\chi^{(1)}$, $\chi^{(2)}$ and $\chi^{(3)}$, all depend on frequencies.

The second class of nonlinearities are those which involve excitation of a medium. The excitation in turn modifies the laser propagation. In this class of nonlinear optical behaviour, saturation of absorption is the·commonest example. Both types of nonlinearities have been observed in fullerenes and sometimes they interfere with each other. One very common example where this happens is the Degenerate Four Wave Mixing ( DFWM )
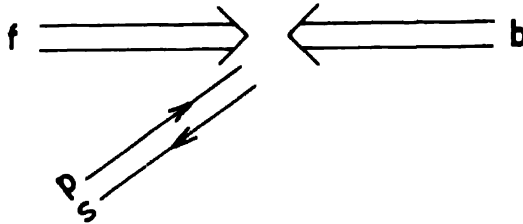


**Figure 5.** Degenerate four wave mixing.

depicted schematically in Figure 5. If the medium is nonabsorbing the output or signal beam (wave vector $k_s = -k_p$) can be produced by the nonlinear polarization

$$P^{\text{NLS}}(\omega) = \chi^{(3)} E_f(\omega) E_p^*(\omega) E_b(\omega) \exp\{i(k_f - k_p + k_b).r\} \tag{13}$$

where $E_f(\omega)$ is the Fourier component at frequency $\omega$ of the forward pump beam $f$ and similarly for backward pump beam $b$ and the probe beam $p$. The nonlinear source polarization vanishes when any of the three input fields vanishes or when the corresponding susceptibility tensor vanishes. However, if the medium absorbs the incident radiation, a very strong signal can be observed because of the second type of nonlinearities. Consider, for instance, the situation in which the forward pump ($f$) and the probe beams are incident simultaneously. They will interfere and form an intensity pattern with a period $= 2\pi/|k_f - k_p|$. If the medium can be excited, this intensity grating which will last till the excited medium returns to the ground state or in the some cases only till the excitation becomes uniform because of diffusion of the excited species. As long as the excitation grating lasts, it will be able to diffract the backward beam into the signal beam because the excitation grating is equivalent to a phase grating since the excited medium has a different refractive index. In principle, such an effect is always present as inelastic scattering of light will always excite a medium. However, the effect is strong only when the medium has noticeable absorption. If our aim is to measure the nonlinear susceptibility due to electronic polarization of the medium, these effects are a nuisance since they can give false signals. On the other hand, for many application these effects can be very important because they are large and can be observed with low power lasers.

Several DFWM experiments have been performed on fullerenes with widely differing results. The first report by Blau *et al* [62] unfortunately suffered from some incorrect analysis of the data. Similar experiments using a Q–switched Nd : YAG laser as the source and $C_{60}$

solution in toluence give $\gamma = 1.6 \times 10^{-31}$ esu, quite close to the value $6 \times 10^{-32}$ esu obtained be reanalysing the data given by Blau *et al* for $C_{60}$ solution in benzene. These values are, however, much higher than those reported by Kafafi *et al* [63], who using thin film samples found $\gamma = 3.10^{-34}$ esu for $C_{60}$ using a mode locked Nd : YAG laser with a pulse width of 35 ps. They also found that at intensities $\geq$ 1GW/cm$^2$ a fifth order process started to contribute significantly. They repeated [64] DFWM experiments on $\leq .5$g / L solutions of $C_{60}$ in benzene and found that the DFWM signal was indistinguishable from that for pure benzene. They concluded that a contribution to $\chi^{(3)}$ from $C_{60}$ should not be observable in any of the benzene solutions used by Blau *et al*. Similar comments should be valid for the results of Gong *et al* [65] and to the large value of $\chi^{(3)}$ for $C_{70}$ solution in toluene obtained by Yang *et al* [66] using the same arrangement. As already noted, DFWM signal can come from the creation of an excitation grating and such a contribution will be sensitive to the pulse duration. However, a satisfactory explanation is still awaited. Even in the experiments of Kafafi *et al*, the role of two–photon resonant contribution could be important since for the ratio $\chi_{xyxy}^{(3)} / \chi_{xxxx}^{(3)}$ they measure a value $\approx 1/7$ instead of the value of 1/3 expected for nonresonant response [67] for a molecule with icosahedral symmetry. This group also measured the resonant DFWM response in thin films of $C_{60}$ and $C_{70}$ [68] using a picosecond tunable dye laser. They find that at 597 nm and 675 nm, DFWM from $C_{60}$ and $C_{70}$ thin films is large and is dominated by excited state population observing $\chi^{(3)}$ as large as $2.1 \times 10^{-9}$ esu in $C_{70}$ at 597 nm. There are two components in the time resolved DFWM—one fast component apparently corresponding to population in the $S_1$ state and other a slow part corresponding to population in the $T_1$ state. Using 150 fs pulses at 633 nm, Rosker *et al* [69] also measured time resolved DFWM on $C_{60}$ and $C_{70}$ thin films on quartz. They estimate $\chi^{(3)} \approx 2 \times 10^{-10}$ esu for $C_{60}$. Since $C_{60}$ films absorb much more at 633 nm than at 1064 nm, it is qualitatively reasonable that this value of $\chi^{(3)}$ is much more than that reported by Kafafi *et al*. However, by the same token the value of $\chi^{(3)}$ for $C_{70}$ should be much more than the value $3 \times 10^{-10}$ esu reported by them. Their time resolved investigation showed that there are 3 regimes in the decay of gratings. The fastest components is faster than their pulse auto–correlation and can be attributed to the electronic polarization, the next component has a large amplitude and a decay constant of 0.2 ps and a still slower one with a decay constant of few ps. The nature of these decay mechanisms could not be resolved. From the point of view of practical utility of fullerenes, it is clear that they promise quite large and fast response. It is the accumulation of population in the triplet state that has to be avoided somehow. In another interesting experiment Zhang *et al* [70] measured the DFWM from $C_{60}$ and $C_{70}$ solutions in toluene using 30 ps pulses at 532 nm. They avoided the effects due to thermal gratings and other long lived gratings by making the probe beam polarization perpendicular to the two pump beams. They estimate $\gamma_{xyxy} \approx 2 \times 10^{-30}$ esu for $C_{60}$ and an amazingly large $\gamma_{xyxy} \approx 10^{-26}$ esu for $C_{70}$ with the sign of $\gamma_{xyxy}$ for $C_{70}$ being opposite of that for toluene. These results appear quite difficult to reconcile with those of Kafafi *et al*. Although no estimates for experimental accuracy are given the error could be large for $C_{60}$ since the $\chi^{(3)}$ for solution differs very

little over the range of concentration studied. Critical reexamination of these results appears necessary. Interestingly, using 10 ns pulses at 532 nm, the DFWM experiments of Vijaya *et al* [71] gave $\chi^{(3)} \approx 10^{-27}$ esu, much larger than even the results of Zhang *et al*. Even when the probe beam is cross polarized to the two pump beams, the DFWM reflectivity drops only by about a factor of 5 or 6 so that a simple thermal contribution is ruled out. However, the order of magnitude of the thermal contribution was estimated to be in rather good agreement with the observed result.

In contrast to DFWM, second and third harmonic generation is directly related to the electronic polarization of the medium. Being inversion symmetric molecules, $C_{60}$ or its solid form are expected to show negligible second harmonic generation. In the first experimental observation of nonlinear optical response of a 600 Å thick film of $C_{60}$ on silica, Hoshi *et al* [72] looked for the second and third harmonic generation of a Nd : YAG laser. Some second harmonic was observed—however, the generated signal was too weak to do any detailed analysis. The third harmonic signal was compared with that form a 200 Å thick single crystalline epitaxial film fluoro–bridged aluminium phthalocyanine polymer on KBr and a $\chi^{(3)} = 2 \times 10^{-10}$ esu was estimated for the $C_{60}$ film. Later experiments by Kajzar *et al* [73] used silica substrate itself as a standard and estimated $\chi^{(3)} = 8.2 \times 10^{-11}$ esu. This value is estimated to be enhanced due to resonance at $3\omega$. Kajzar *et al* also measured the dispersion of $\chi^{(3)}$ $(-3\omega, \omega, \omega, \omega)$ and found that $\left|\chi^{(3)}\right|$ shows fairly strong resonance in region 250 nm $< \lambda/3 < 500$ nm. Similar results have been reported by Meth *et al* [74]. However, their values appear to be smaller than those of Kajzar *et al* although both used the same standard value of $\chi^{(3)}$ for silica at 1.9 $\mu$m fundamental wavelength. More recently Neher *et al* [75] have also reported third harmonic generation from $C_{60}$ and $C_{70}$ solutions in toluene at three wavelengths—1064 nm, 1500 nm and 2000 nm. Interestingly they found that at these 3 wavelengths, the real and imaginary parts of $\gamma$ did exhibit a strong dispersion. Apparently somemore work is needed to reconcile these results with those of Meth *et al* and Kajzar *et al*. Also needing further investigation is the second harmonic generation from $C_{60}$ films— observed first by Hoshi *et al* and later reinvestigated in detail by Wang *et al* [76]. They observed a strongly temperature dependent SHG from Corona poled films with maximum value of $10^{-8}$ esu at 140 C. This is larger than the value at room temperature by about a factor of 10. Among other explanations of their results one possibility mentioned by Wang *et al* is the formation of $C_{60}O$ because of the presence of oxygen in their film as shown by Auger spectroscopy.

The fact that the HOMO–LUMO transition is forbidden by symmetry in $C_{60}$ makes it an almost ideal reverse saturable absorber. Over a rather wide spectral range, the absorption from the excited state is much more than from the ground state. Exploiting this Tutt and Kost [77], have shown that this molecule is attractive for use in an optical limiter *i.e.*, a device which has a high transparency at low intensities and high opacity at high intensities. Such devices are very important for protecting sensitive optical detectors against damage by

unintended exposure to a high intensity source. More recently, Joshi *et al* [78] from our group investigated the optical limiting by $C_{60}$ solution in toluene arfd have shown that reverse saturable absorption is not sufficient to explain the optical limiting behaviour of this medium. In fact, multi–photon absorption from the excited state or another nonlinearity has to be invoked to explain the intensity dependent transmission of $C_{60}$ quantitatively [79].

So far, we have described only the experiments on $C_{60}$ and $C_{70}$. However, Wang and Cheng [80] have reported dc electric field second harmonic generation in fullerene/N,N-diethylaniline (DEA) charge transfer complex. For $C_{60}$/DEA Complex they find the dipole projection of $\beta$ as $6.7 \times 10^{-29}$ esu.

## 6. Hyperpolarizability calculations

Initial motivation for the study of optical nonlinearities in fullerenes came from the fact that $\pi$–electron systems are well known to have large nonlinearities in one and two dimensions [81–84]. The early attempts were therefore directed to obtain reliable estimates of hyperpolarizabilities of fullerenes to determine their potential as nonlinear optical materials. A second more fundamental reason has emerged during such studies. Because of their hollow cage structure and highly polarizable $\pi$–electron cloud (recall that the refractive index for $C_{60}$ solid is > 2, although its density is less than half that of diamond) they provide a challenging opportunity to test our understanding of electromagnetic response of many electron systems.

In principle, once the electronic eigenstates of a system are known, atleast the nonresonant or weakly resonant response of the system can be easily calculated using the standard expressions obtained by time–dependent perturbation theory. But the electronic eigen states are known only approximately and it is possible that an approximation which is quite adequate for the description of linear optical response is highly inadequate for describing nonlinear response. For the ground state, the most reliable information that we can obtain so far is the self–consistent one–electron states in the local density approximation wherein each electron moves in a self consistent potential generated by all the electrons. In the presence of an electrostatic field, the ground state problem can again be solved self–consistently and from these solutions one can get the hyperpolarizabilities as $\omega \to 0$. However, information about the excited states and hence the linear and nonlinear optical spectra of the molecules is usually obtained under the assumption that self consistent potential does not change on excitation. Using the one–electron eigenstates one can also calculate the frequency dependent linear and nonlinear polarizabilities. In most molecules the zero frequency limit of these polarizabilities is close enough to the above mentioned self consistent ground state calculations. As we will see, this does not seem to be so for fullerenes—and hence the challenge!

Independent of the method of calculation, the various components of the polarizability tensours $\alpha$, $\beta$ and $\gamma$ are related to each other by symmetry. The symmetry groups of $C_{60}$ is $I_h$

and that of $C_{70}$ is $D_{5h}$. Both these point groups are not among the crystallographic point groups and are thus not included in the standard tables of symmetry relations for nonlinear polarizabilities [61,85]. We have determined the symmetry properties of the linear and nonlinear electric dipole polarizability tensors $\alpha$, $\beta$, and $\gamma$ for these two symmetry groups *viz.*, $I_h$ and $D_{5h}$. We find that $\alpha$ and $\gamma$ for $C_{60}$ ($I_h$ group) have structures identical to those of an isotropic system while for $C_{70}$ ($D_{5h}$ group) they behave like those for an inversion symmetric hexagonal system of $D_{6h}$ symmetry. Surprisingly $\beta$ vanishes for $D_{5h}$ symmetry although this group does not contain inversion symmetry. In contrast, for all the 21 non-centrosymmetric crystallographic point groups at least one component of $\beta$ is nonvanishing by symmetry. For $C_{70}$, $\gamma$ has 21 non-zero components with 10 of them independent. They are,

$$\gamma_{xxxx} = \gamma_{yyyy} ; \qquad \gamma_{zzzz}$$

$$\gamma_{xxyy} = \gamma_{yyxx}$$

$$\gamma_{xyyx} = \gamma_{yxxy}$$

$$\gamma_{xyxy} = \gamma_{yxyx}$$

$$\gamma_{xxxx} = \gamma_{xxyy} + \gamma_{xyyx} + \gamma_{xyxy}$$

$$\gamma_{xxzz} = \gamma_{yyzz} ; \qquad \gamma_{zzxx} = \gamma_{zzyy}$$

$$\gamma_{xzzx} = \gamma_{yzzy} ; \qquad \gamma_{zxxz} = \gamma_{zyyz}$$

$$\gamma_{xzxz} = \gamma_{yzyz} ; \qquad \gamma_{zxzx} = \gamma_{zyzy} \qquad\qquad (14)$$

This structure is identical to that for the hexagonal classes $D_6$ (622), $C_{6v}$ (6mm), $D_{6h}$ (6/mmm) and $D_{3h}$ ($\overline{6}2$m) [61,85].

One may note that under Kleinman symmetry [61] (*i.e.*, invariance under permutation of all the suffixes), which is appropriate for a dispersion free situation, only three components of $\gamma$ are independent which may be taken to be $\gamma_{xxxx}$, $\gamma_{zzzz}$ and $\gamma_{xxzz}$. All the other components may be obtained from these by permutation of the suffixes, interchange of $x$ and $y$ and using the relation $\gamma_{yyyy} = \gamma_{xxxx} = 3\gamma_{xxyy}$.

All the odd rank tensors are zero for $I_h$ symmetry as it contains the inversion operation. We found that $\alpha_{xx} = \alpha_{yy} = \alpha_{zz}$, *i.e.*, same as for an isotropic or a cubic material, and $\gamma$ has 21 non-zero components, of which only 3 are independent. They are

$$\gamma_{xxxx} = \gamma_{yyyy} = \gamma_{zzzz}$$

$$\gamma_{xxyy} = \gamma_{yyxx} = \gamma_{yyzz} = \gamma_{zzyy} = \gamma_{zzxx} = \gamma_{xxzz}$$

$$\gamma_{xyyx} = \gamma_{yxxy} = \gamma_{yzzy} = \gamma_{zyyz} = \gamma_{zxxz} = \gamma_{xzzx}$$

$$\gamma_{xyxy} = \gamma_{yxyx} = \gamma_{yzyz} = \gamma_{zyzy} = \gamma_{zxzx} = \gamma_{xzxz}$$

$$\gamma_{xxxx} = \gamma_{xxyy} + \gamma_{xyxy} + \gamma_{xyyx} . \qquad\qquad (15)$$

This structure is identical to that for an isotropic material. Under Kleinman symmetry only one component is independent with $\gamma_{xxxx} = 3\gamma_{xxyy}$ and all the components related by an interchange or permutation of $x$, $y$, $z$ are equal. We note that this is exactly valid for the static (zero–frequency) polarizabilities and provides a check on the theoretical calculations.

The fact that $\gamma$ of $C_{60}$ has the same structure as that for an isotropic material, implies that all the symmetry imposed selection rules for third order nonlinear optical processes in isotropic materials will apply to $C_{60}$ as well. As a consequence, we suggested that third harmonic generation experiments can be used to probe solid state effects on the electron density of solid $C_{60}$. This possibility arises because $C_{60}$ forms a molecular solid so that one would expect that its nonlinear susceptibility $\chi^{(3)}$ can be obtained as a sum of the $\gamma$ of the individual molecules to a good approximation. Thus for solid $C_{60}$, although only those symmetry restrictions on $\chi^{(3)}$ demanded by its cubic crystallographic point group are strictly valid, $\chi^{(3)}$ will be isotropic to a good degree of accuracy. Thus the deviation from isotropy of $\chi^{(3)}$ of solid $C_{60}$ will give a measure of the inter–molecular interactions. In particular, since third harmonic generation from an isotropic medium vanishes for circularly polarized light [86], the ratio of the third harmonic generated by circularly and linearly polarized light in $C_{60}$ solid will give a measure of the cubic perturbation of the molecular electron density due to inter–molecular interactions.

Using the electronic states obtained in the pseudopotential model for $C_{60}$ and the tight binding method for $C_{59}B$ and $C_{59}N$ we have calculated their electric–dipole susceptibilities. For this we diagonalized the hamiltonian including the interaction term $ezE_z$ and calculated the induced changes in the total energy or the dipole moment as a function of the field. The sum–over–states method was also used as a check and for estimating the effect of dispersion. In obtaining the expressions for the sum–over–states method, care was taken to include all the diagonal matrix elements of the displacement $z$ which will generally be nonzero in systems lacking inversion symmetry. For the $s$–$p$ atomic dipole matrix element in the tight binding method [56], we used 0.5 Å throughout. The energy and dipole moment expansions in terms of $E_z$ both give numerically indistinguishable results for the polarizabilities. Our calculated results are shown in Table 1.

It is interesting to note several points here. First we compare the numbers for $C_{60}$ with those for a one dimensional $\pi$–electron system : $\beta$–carotene with 22 $\pi$–electrons delocalized over a zig–zag chain of about 24 bond lengths. For $\beta$–carotene, the calculated values for the polarizabilities, in the free–electron model [81] are : $\alpha_{zz} = 1.8 \times 10^{-22} \, cm^3$ and $\gamma_{zzzz} = 4.8 \times 10^{-33}$ esu where z is the molecular axis. The contributions of $\alpha_{yy}$, $\alpha_{zz}$, $\gamma_{yyyy}$ and $\gamma_{zzzz}$ are expected to be much smaller because the $\pi$–electron extension perpendicular to the molecular axis is much smaller. Thus we may approximate $\langle\alpha\rangle \simeq \alpha_{zz}/3 = 60 \, Å^3$ so that $\langle\alpha\rangle/N_\pi$, the linear polarizability per $\pi$–electron is nearly the same for the two molecules. In contrast $\langle\gamma\rangle/N_\pi$ is much smaller for $C_{60}$. This is partly because $\gamma$ increases steeply with increasing delocalization length and one–dimensional $\pi$–electron system provides a larger conjugation

length per $\pi$–electron. From this view point, tubules would be the preferred $\pi$–electron systems. However, electronic structure of such molecules is still not well understood.

**Table 1.** The calculated values of the dipole–moments and polarizabilities of $C_{60}$, $C_{59}B$ and $C_{59}$.

| | $C_{60}$ | | | $C_{59}B$ | | $C_{59}N$ |
|---|---|---|---|---|---|---|
| | (a) | (b) | (c) | (d) | (e) | |
| Dipole moment $(10^{-18}$ esu) | . | .. | . | -9.54 | -6 3 | 10.8 |
| $\alpha (10^{-24}$ esu) | 180 | 195 *215* | 213 | 340 | 314 | 354 |
| $\beta (10^{-30}$ esu) | .. | . | .. | -1023 | -1100 | 1372 |
| $\gamma (10^{-36}$ esu) | 130 | 349 *346* | 508 | 269 | 8112 | -4860 |

(a)    E P M results. Ref [43]
(b)    $d_1 = 1.369$ Å ; $d_2 = 1 453$ Å. Values in italics from Ref. [50]
(c)    $d_1 = 1.40$ Å , $d_2 = 1.45$ Å
(d)    $d_1 = 1 40$ Å ; $d_2 = 1.45$ Å for all atoms.
(e)    extended carbon–boron bonds (see text)

Secondly, the hyperpolarizability of $C_{60}$ is also reduced by the high symmetry of the molecule and consequent selection rules as well as the fact that the HOMO–LUMO transition is parity forbidden. This indicates that adding electrons to the $t_{1u}$ (LUMO) state as in $C_{59}N$ or $C_{60}^-$ or removing electrons from the $h_u$ (HOMO) state as in $C_{59}B$ or $C_{60}^+$ will increase $\gamma$. Our tight–binding calculations for $C_{59}B$ and $C_{59}N$ indeed confirm this. Thus as for symmetric cyanines, perturbation of a $\pi$–electron system by chemical substitution appears to be an effective means of increasing the hyperpolarizability of a system if it is much below that of other equally polarizable systems.

Further, the lack of inversion symmetry allows the doped molecules to have an electric dipole moment which is negative in $C_{59}B$ and positive in $C_{59}N$. The dipole moment is not sensitive to the difference between the long and short C–C bond lengths but does reduce noticeably when boron is moved out in $C_{59}B$. Our values for the dipole moment are about five times larger than those reported in Ref. 53. Secondly the tight–binding results for $\alpha$ and $\gamma$ are sensitive to the difference in the long and short bond lengths. In particular, $\gamma$ increases by 46% when the more realistic, experimentally determined, bond lengths are used. For boron displaced structure of $C_{59}B$ we calculate relatively high nonresonant $\gamma \approx 8 \times 10^{-33}$ esu. This is found to be ~ 30 times larger than that estimated for the same molecule if the atomic positions are assumed to be same as in $C_{60}$. This indicates that an agreement between various calculations of $\gamma$ to within a factor of 2 may be considered satisfactory. Thus the empirical

pseudopotential method and the tight–binding method both provide results in reasonable agreement with each other.

Finally, we note that in doped fullerenes, the hyperpolarizability $\beta$ is large and relatively insensitive to the atomic positions. The main contribution to $\beta$ comes from two split-off impurity levels—the split-off $h_u$ and $g_g$ levels in $C_{59}B$ and the split-off $t_{1u}$ and $t_{1g}$ levels in $C_{59}N$. These $\beta$ values are comparable to the largest reported for organic molecules. Using the density and the local field correction corresponding to the solid $C_{60}$, this value of $\beta$ corresponds to a nonlinear susceptibility $\chi^{(2)}$ of $\approx 10^{-5}$ esu for both $C_{59}B$ and $C_{59}N$.

Interestingly, while in the one–dimensional case the HOMO–LUMO gap is strongly affected by the bond alternation, for $C_{60}$ the gap is not sensitive to bond alternation.

In the above discussion, screening due to electron–electron interaction has not been considered and all the polarizability values presented are the unscreened or bare values *i.e.*, it has been assumed that the field seen by electrons in a $C_{60}$ molecule is the same as the one applied to it. In reality this is not so, because when the electron cloud is polarized, it also modifies the charge density and hence the self consistent potential seen by each electron. Bertsch *et al* [56], used the random phase approximation neglecting the radial spread in electron density to estimate that for $C_{60}$ the effect of including this 'screening' correction is to reduce $\alpha$ by a factor of $f = \left(1 + \alpha/R^3\right) \simeq 5$. Nair [43] has also reported a similar calculation using the EPM wavefunctions and found that the screening is very sensitive to the radial spread in the electron density, the screening decreasing with increasing shell thickness. For the linear response, he found that $f \simeq \left(1 + a\,\alpha/R^3\right)$ to a good accuracy where $a$ is a constant which depends on the shell thickness. For $t = 3$ Å, he found $a = 0.73$. It can be much smaller for a more realistic radial density. For $\gamma$, the screening correction was found to be slightly smaller than $f^4$. From the measured refractive index (2.25) of $C_{60}$ thin films, we estimate $\alpha_{screened} \simeq 100$ Å$^3$ using the Claussius–Mossotti relation. With $\alpha_{bare} \simeq 200$ Å$^3$, we estimate the screening factor $f$ to $\simeq 2$ which implies a reduction of $\gamma$ by a factor of 16 from the unscreened values.

It may be argued that unless an accurate understanding of the screening correction can be made, no useful estimate of hyperpolarizability can be made. This is only partially true. The screening corrections in $C_{60}$ and $C_{59}B$ can be expected to be similar. Thus, if the unscreened calculations give $\beta$ and $\gamma$ for $C_{59}B$ a conservative estimate can be made for the ratio of hyperpolarizabilities in the two molecules.

Next, we compare our results with some of the experimental observations. Hoshi *et al* [72] report $\left|\chi^{(3)}_{xxxx}(-3\omega, \omega, \omega, \omega)\right| \simeq 2 \times 10^{-10}$ esu for a thin film. If we assume that the film has near crystalline packing and that Lorentz local field correction is applicable, we obtain $\gamma_{zzz} \simeq 4 \times 10^{-33}$ esu. This is larger than our calculated (in EPM) value by a factor of about 30 which could be attributed to resonant enhancement of $\gamma$ since, in their experiment, 2 $\hbar\omega$ and 3 $\hbar\omega$ are both close to resonance. To check this, we used our calculated electric dipole matrix

elements and energies to estimate the frequency dependence of $\alpha(\omega)$ and $\gamma(\omega_1, \omega_2, \omega_3)$. For $\gamma(\omega, \omega, \omega)$ measured by Hoshi *et al* [72] we find an enhancement by a factor of 16 for 3 $\hbar\omega$ about 0.1 eV away from the 3-photon allowed transition at 3.7 eV in our calculation. We also estimate that the enhancement is relatively smaller near the two-photon resonance at 1.82 eV. The calculated values of $\gamma_{\text{bare}}$ are also in good agreement with those measured by nonresonant DFWM [63] and third harmonic generation [73]. In the meanwhile, several other calculations of hyperpolarizabilities have been reported [87–91]. Generally, all calculations ignoring screening give similar results which are more or less in agreement with each other and the relevant experimental data. The calculations including screening always give very much lower values of $\gamma$. Admittedly, much better understanding of screening in $C_{60}$ is required before meaningful comparison of the absolute values of $\chi^{(3)}$ can be made. Since the screening is very sensitive to the spill over of the electron density, it is possible that intra–molecular screening is also strongly influenced by intermolecular interactions. This would lead to different effective values in different solvents.

## 7. Conclusion

I have presented a critical assessment of the limited information available about the nonlinear optical properties of fullerenes. The results available so far certainly indicate the great potential of this family of molecules as nonlinear optical materials. The experimental results are not yet fully consistent with each other. Theoretically, the most important unsolved problem is the evaluation of the apparently rather large intramolecular screening. In particular, the understanding of how this screening affects the nonlinear optical response appears inadequate. Although it appears unlikely, the dispersion of $\chi^{(3)}$ being the source of the discrepancy, should be and can be ruled out by more experimental measurements. Other experimental measurements which are expected to throw more light on this, are the comparison of one photon and multiphoton spectra. Quantitative analysis of even linear optical absorption spectra is still inadequate, particularly with regard to the role of screening. Also desirable are data on the highest transparency that can be achieved in the condensed state since residual absorption is a major concern in organics [92]. Finally, we note that a great deal can be learnt from the spectroscopy of rare earth atoms encapsulated in the highly polarizable cage provided by fullerenes.

## Acknowledgment

### References

[1]    W Krätschmer, L D Lamb, K Fostiropoulos and D R Huffman 1990 *Nature* **347** 354

[2]    H W Kroto, J R Heath, S C O'Brien, R F.Curl and R E Smalley 1985 *Nature* **318** 162

[3]   H W Kroto, A W Allaf and S P Balm 1991 *Chem. Rev.* **91** 1213

[4]   R F Curl and R E Smalley 1991 *Sci. Am.* **265** 54

[5]   D R Huffmann 1991 *Phys. Today* **45**(11), 22(Nov)

[6]   W Krätschmer 1991 *Z. Phys.* **D19** 405

[7]   J Baggot 1991 *New Scientist* **131** 34 (6 July)

[8]   W D Knight, K Clemenger, W A deHeer, W A Saunders, M Y Chou and M L Cohen 1984 *Phys. Rev. Lett.* **52** 2141

[9]   See e.g., T Bergmann, H Limberger and T P Martin 1988 *Phys. Rev. Lett.* **60** 1767

[10]  J L Martins, R Car and J Buttet 1981 *Surf. Sci.* **106** 265

[11]  G Meijer and D S Bethune 1990 *J. Chem. Phys.* **93** 7800

[12]  A W Castleman, Jr B Guo and S Wei in Ref. [13]

[13]  V Kumar, T P Martin and E Tosatti eds 1993 *Clusters and fullerenes* (Singapore : World Scientific)

[14]  G S Hammond and V J Kuck (eds) 1992 *Fullerenes, A C S symposium series* **481**, (Washington DC : Am. Chem. Soc.)

[15]  C Taliani and G Ruani (eds.) 1993 *Fullerenes : Status and Perspectives* (Singapore : World Scientific)

[16]  (a) *Accounts Chem. Research* 1992 **25** (3); (b) *Carbon* 1992 **6** (8); (c) *Indian J. Chem.* 1992 **31A & B**; (d) *J. Phys. Chem. Sol.* 1992 **53** (12); (e) *Appl. Phys. A* 1993 **56** (3)

[17]  H R Krishnamurthy and A K Sood 1992 *Rev Sol. St Science* **5** 587

[18]  R L Whetten in Ref. 16(a)

[19]  W·A Scrivens, P V Bedworth and J M Tour 1992 *J. Am. Chem. Soc.* **114** 7917

[20]  R E Smalley in Ref. [15]

[21]  See e.g., A F Hebard 1992 *Phys. Today* **46** 26, K Holczer in Ref. [13]

[22]  T Pradeep, V Vijayakrishnan, A K Santra and C N R Rao 1991 *J. Phys. Chem.* **95** 10564

[23]  F Wudl in Ref [16(a)]

[24]  W I F David, R M Ibberson, J C Matthewman, K Prassides, T J S Dennis, J P Hare, H W Kroto, R Taylor and D R M Walton 1991 *Nature* **353** 147

[25]  C S Yannoni, P P Bernier, D S Bethune, G Meijer and J R Salem 1991 *J. Am Chem. Soc.* **113** 3190

[26]  B P Feuston, W Andreoni, M Parrinello and E Clementi 1991 *Phys. Rev.* **B44** 4056

[27]  R Car and M Parrinello 1985 *Phys. Rev Lett.* **55** 2471

[28]  D R McKenzie, C A Davis, D J H Cockayne, D A Muller and A M Vassallo 1992 *Nature* **355** 622

[29]  W Andreoni, F Gygi and M Parrinello 1991 *Chem. Phys. Lett.* **189** 241

[30]  S Saito and A Oshiyama 1991 *Phys. Rev.* **B44** 11532

[31]  C Z Wang, C T Chan and K M Ho 1992 *Phys. Rev.* **B46** 9761

[32]  K Kikuchi, N Nakahara, T Wakabayashi, S Suzuki, H Shiromaru, Y Miyake, K Sato, I Ikemoto, M Kainosho and Y Achiba 1992 *Nature* **357** 142

[33]  F Diederich, R L Whetten, C Thilgen, R Ettl, I Chao, M M Alvarez 1991 *Science* **254** 1768

[34]  X Q Wang, C Z Wang, B L Zhang and K M Ho 1992 *Phys. Rev. Lett.* **69** 69

[35]  P A Heiney, J E Fischer, A R McGhie, W J Romanow, A M Denenstein, J P McCauly, Jr., A B Smith III and D E Cox 1991 *Phys. Rev. Lett.* **66** 2911 ; R Sachidanandam and A B Harris 1991 *Phys. Rev. Lett.* **67** 1467

[36]  J P Lu, X P Li and R M Martin 1992 *Phys. Rev. Lett.* **68** 1551

[37]  P H M Vanloosoreccht, P J M Vanbentum and G Meijer 1992 *Phys. Rev. Lett.* **68** · 1176 ; N Chandrabhas, K Jayaraman, D V S Mutthu, A K Sood, R Seshadri and C N R Rao 1993 *Phys. Rev.* **B47** 10963 ; V Verma, R Seshadri, A Govindaraj, A K Sood and C N R Rao 1993 *Chem. Phys. Lett.* **203** 545

[38]  R C Haddon, L E Brus and K Raghavachari 1986 *Chem. Phys. Lett.* **125** 459

[39]     S Larsson, A Volosov and A Rosen 1987 *Chem. Phys. Lett* **137** 501

[40]     S Satpathy 1986 *Chem. Phys Lett.* **130** 545

[41]     K Fostiropolous in Ref [13]

[42]     S V Nair and K C Rustagi 1991 *Proc. Solid State Phys. Symp. Banaras Dec 1991* (Dept. Atomic Energy, Bombay 1991) **Vol 34C** p98 , K C Rustagi, L M Ramaniah and S V Nair in Ref. [13]

[43]     S V Nair 1993 *Ph D Thesis* (D A University, Indore, India)

[44]     G A Gallup 1991 *Chem. Phys. Lett.* **187** 187

[45]     See e.g. M L Cohen and J R Chelikowsky 1988 *Electronic Structure and Optical Properties of Semiconductors* (Berlin : Springer–Verlag)

[46]     K Yabana and G Bertsch, Michigan University preprint

[47]     W G Harter and D E Weeks 1989 *J. Chem. Phys* **90** 4727

[48]     D Tománek and M A Schluter 1991 *Phys Rev. Lett.* **67** 2331

[49]     M Menon and K R Subbaswamy 1991 *Phys. Rev Lett.* **67** 3487

[50]     Y Wang, G Bertsch and D Tománek 1991 *Z. Phys.* **D25** 181

[51]     W A Harrison 1980 *Electronic Structure and the properties of Solids : The Physics of the Chemical Bond* (San Francisco : Freeman)

[52]     L M Ramaniah, S V Nair and K C Rustagi *Opt Commun.* (submitted)

[53]     W Andreoni, F Gygi and M Parrinello 1992 *Chem. Phys. Lett.* **190** 159

[54]     H Ajie, M M Alvarez, S J Anz, R D Beck, F Diederich, K Fostiropoulos, D R Huffman, W Kratschmer, Y Rubin, K E Schriver, D Sensharma and R L Whetten 1990 *J Phys Chem.* **94** 8630

[55]     S Leach, M Vervloet, A Despres, E Breheret, J P Hare, T J Dennis, H W Kroto, R Taylor and D R M Walton 1992 *Chem. Phys.* **160** 451

[56]     F Bertsch, A Bulgac, D Tománek and Y Wang 1991 *Phys. Rev Lett.* **67** 2690

[57]     H Steger, J de Vries, B Weisser, C Menzel, B Kamke, W Kamke and I V Hertel (to be published)

[58]     P N Saeta, B I Greene, A R Kortan, N Kopylov and F A Thiel 1992 *Chem Phys Lett* **190** 184

[59]     J H Weaver, J L Martins, T Komeda, Y Chen, T R Ohno, G H Kroll, N Troullier, R E Haufler and R E Smalley 1991 *Phys Rev Lett* **66** 1741

[60]     Y R Shen 1984 *Principles of Nonlinear Optics* (New York : Wiley)

[61]     C Flytzanis 1975 in *Quantum Electronics · A Treatise* **Vol I** eds. H Rabin and C L Tang (New York Academic)

[62]     W J Blau, H J Byrne, D J Cardin, T J Dennis, J P Hare, H W Kroto, R Taylor and D R M Walton 1991 *Phys. Rev. Lett.* **67** 1423. From Figure 2 of this paper, we estimate $\gamma$ ($C_{60}$) / $\gamma$ (Benzene) $\simeq 1.7 \times 10^4$ which implies $\gamma(C_{60}) \simeq 6 \times 10^{-32}$ esu. This is much smaller than the value claimed in this paper

[63]     H Kafafi, J R Lindle, R G S Pong, F J Bartoli, L J Lingg and J Milliken 1992 *Chem. Phys. Lett.* **188** 492

[64]     Z H Kafafi, F J Bartoli, J R Lindle and R G S Pong 1992 *Phys. Rev Lett.* **68** 2705

[65]     Q Gong, Y Sun, Z Xia, Y H Zou, Z Gu, X Zhou and D Qiang 1992 *J. Appl. Phys.* **71** 3025

[66]     S C Yang, Q Gong, Z Xia, Y H Zhou, Y Q Wu, D Qiang, Y L Sun and Z N Gu 1992 *Appl. Phys.* **B55** 51

[67]     L M Ramaniah, S V Nair and K C Rustagi 1993 *Opt. Commun* **96** 289

[68]     S R Flom, R G S Pong, F J Bartoli and Z H Kafafi 1992 *Phys Rev.* **B46** 15598

[69]     M J Rosker, H O Marcy, T Y Chang, J T Khoury, K Hnasen and R L Whetten 1992 *Chem. Phys. Lett.* **196** 427

[70]     Z Zhang, D Wang, P Ye, Y Li, P Wu and D Zhu 1992 *Opt. Lett.* **17** 973

[71]     R Vijaya, Y V G S Murti, G Sundararajan, C K Mathews and P R Vasudeva Rao 1992 *Opt. Commun.* **94** 353

[72]  H Hoshi, N Nakamura, Y Maruyama, T Nakagawa, S Suzuki, H Shiromaru and Y Achiba 1991 *Jpn. J. Appl. Phys. Lett.* **30** L 1397

[73]  F Kajzar, C Taliani, R Zamboni, S Rossini and R Danieli in Ref. [14]

[74]  J S Meth, H Vanherzeele and Y Wang 1992 *Chem. Phys. Lett.* **197** 26

[75]  D Neher, G I Stegeman, F A Tinker and N Peyghambarian 1992 *Opt Lett.* **17** 1491

[76]  X K Wang, T G Zhang, W P Lin, Z L Sheng, G K Wong, M Kappes, R P H Chang and J B Ketterson 1992 *Appl. Phys. Lett.* **60** 810

[77]  L W Tutt and A Kost 1992 *Nature* **356** 225

[78]  M P Joshi, S R Mishra, H S Rawat, S C Mehedale and K C Rustagi 1993 *Appl Phys. Lett.* **62** 1763

[79]  S R Mishra, H S Rawat, M P Joshi, S C Mehedale and K C Rustagi (to be published)

[80]  Y Wang and L T Cheng 1992 *J. Phys Chem* **96** 1530

[81]  K C Rustagi and J Ducuing 1974 *Opt. Commun.* **10** 258

[82]  S C Mehendale and K C Rustagi 1979 *Opt Commun.* **28** 359

[83]  See e.g., D S Chemla and J Zyss 1987 (eds.) *Nonlinear Optical Properties of Organic Molecules and Crystals* (Orlando · Academic) , G T Boyd 1989 *J Opt Soc. Am.* **B6** 685 and references there in

[84]  P N Prasad and D J Williams 1991 *Introduction to Nonlinear Optical Effects in Molecules and Polymers* (New York · Wiley)

[85]  P N Butcher 1965 *Nonlinear Optical Phenomena* (Ohio Ohio State University) *For corrections of some errors in Butcher's tables for the third order susceptibility see* Y Zhao 1986 *IEEE J Quant. Elect.* **QE-22** 1012

[86]  P P Bey and H Rabin 1967 *Phys Rev* **162** 794

[87]  G B Talapatra, N Manickam, M Samoc, M E Orczyk, S P Karna and P N Prasad 1992 *J. Phys. Chem.* **96** 5206

[88]  Z Shuai and J L Brédas 1992 *Phys Rev.* **B46** 16135

[89]  A Rosen and E Westin in Ref. [13]

[90]  K Harigaya and S Abe 1992 *Jpn. J Appl Phys.* **31** L887

[91]  N Matsuzawa and D A Dixon 1992 *J. Phys. Chem.* **96** 6872

[92]  B I Green, J Orenstein and S Schmitt-Rink 1990 *Science* **247** 679